Journal of Sensors

Advanced Sensor Application for Energy Data Monitoring and Management Improvement

Lead Guest Editor: Sung-Yong Son
Guest Editors: Eunsung Oh and Bhaskar Krishnamachari

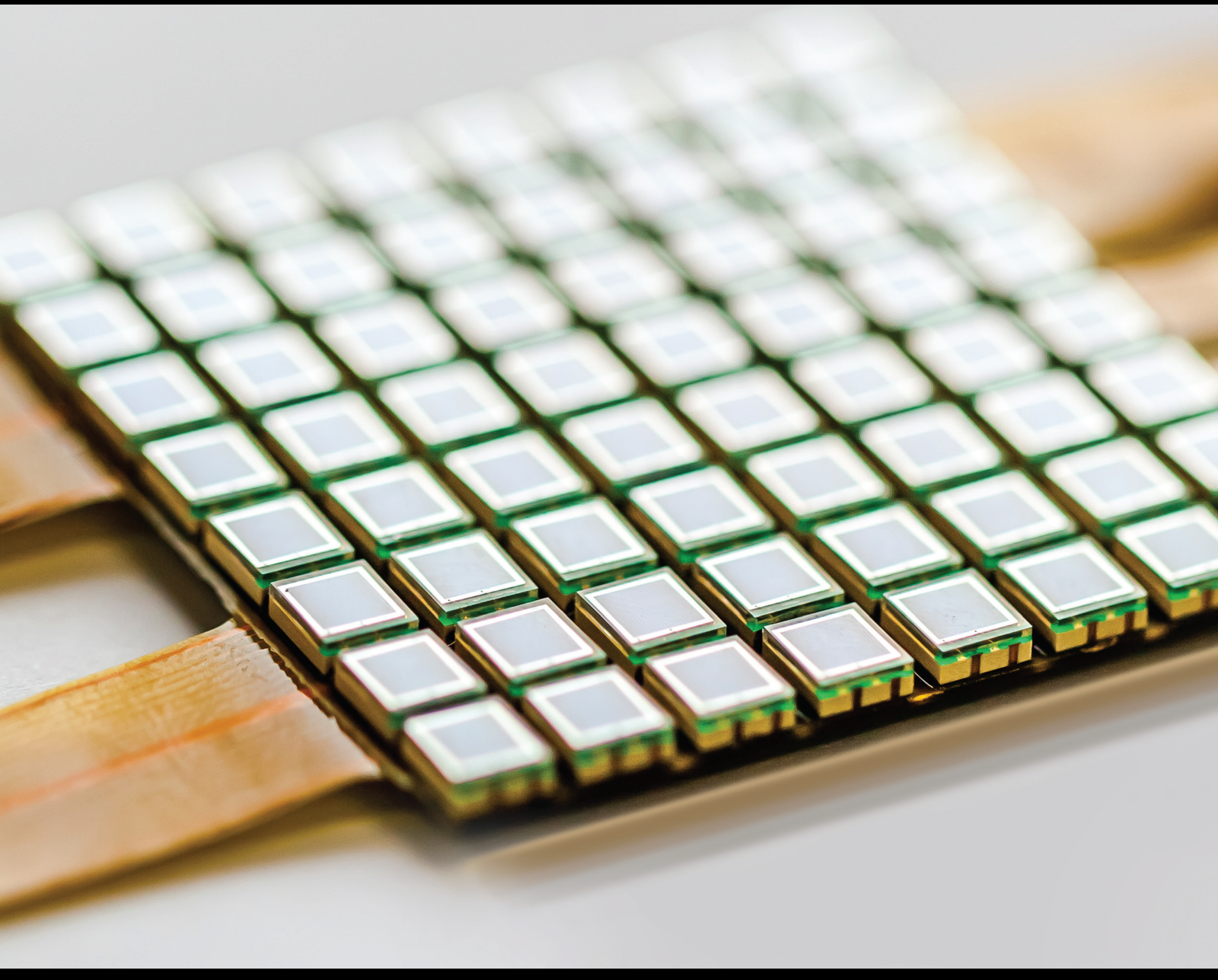

Advanced Sensor Application for Energy Data Monitoring and Management Improvement

Journal of Sensors

Advanced Sensor Application for Energy Data Monitoring and Management Improvement

Lead Guest Editor: Sung-Yong Son
Guest Editors: Eunsung Oh and Bhaskar Krishnamachari

Contents

A Low-Power WLAN CMOS LNA for Wireless Sensor Network Wake-Up Receiver Applications
Mariem Bouraoui, Amel Neifar, Imen Barraj, and Mohamed Masmoudi
Research Article (11 pages), Article ID 7753558, Volume 2023 (2023)

A Novel Routing Protocol for Low-Energy Wireless Sensor Networks
Sebastin Suresh, V. Prabhu, V. Parthasarathy, Rajasekhar Boddu, Yadala Sucharitha, and Gemmachis Teshite
Research Article (8 pages), Article ID 8244176, Volume 2022 (2022)

Hindawi
Journal of Sensors
Volume 2023, Article ID 7753558, 11 pages
https://doi.org/10.1155/2023/7753558

Research Article

A Low-Power WLAN CMOS LNA for Wireless Sensor Network Wake-Up Receiver Applications

Mariem Bouraoui,[1,2] **Amel Neifar**,[2] **Imen Barraj**,[2,3] **and Mohamed Masmoudi**[2]

[1]*National Engineers School of Gabes, University of Gabes, Tunisia*
[2]*Systems Integration and Emerging Energies Laboratory, Electrical Engineering Department, National Engineers School of Sfax, University of Sfax, B.P. 1173, 3038 Sfax, Tunisia*
[3]*Department of Computer Engineering, College of Computer Engineering and Sciences, Prince Sattam bin Abdulaziz University, Al-Kharj 11942, Saudi Arabia*

Correspondence should be addressed to Mariem Bouraoui; mariembr01@gmail.com

Received 12 November 2022; Revised 10 February 2023; Accepted 31 March 2023; Published 5 May 2023

Academic Editor: Eunsung Oh

Wireless communication integration is related to many challenges such as reliability, quality of service, communication range, and energy consumption. As the overall performance of wireless sensor networks (WSN) will be improved if the capacity of each sensor node is optimized, several techniques are used to fine-tune the various circuits of each node. In recent works, the wake-up receiver nodes have been introduced to minimize latencies without increasing energy consumption. To overcome the sensitivity of wake-up receiver limitations, a design of a low-noise amplifier (LNA) with several design specifications is required. This article discusses the relevance of the wake-up receiver in WSN applications and provides a brief study of this component. An LNA design for WSN wake-up receiver applications is presented. The challenging task of the LNA design is to provide equitable trade-off performances such as noise figure, gain, power consumption, impedance matching, and linearity. The LNA circuit is designed for wireless personal area network (WLAN) standards utilizing RF-TSMC CMOS 0.18 μm. Two innovative techniques are applied to the LNA topology to improve its performance: forward body biasing is used to reduce power consumption by 11.43 mW, and substrate resistance is added to reduce noise by 1.8 dB. The developed LNA achieves a noise figure of 1.6 dB and a power gain of 21.7 dB at 5.2 GHz. At 0.6 V, the designed LNA dissipates 0.87 mW.

1. Introduction

The Internet of Things (IoT) is currently at the forefront of converting numerous areas to a degree of smartness by storing and processing data in a distributed manner to increase productivity.

IoT technology is built on powerful wireless devices that are integrated in a complex ecosystem to share and analyze data. These wireless devices are known as sensor nodes, and they are scattered throughout a large network using multiple technologies and communicating at various frequency levels. The operating frequency influences data rate, transmission power, and power consumption in the sensor node.

Wireless technologies such as Wi-Fi, Bluetooth, radio frequency identification (RFID), and ultrawideband (UWB) are used to provide reliable localization in an IoT-based system. As indicated in Figure 1, ultrawideband (UWB) is a digital pulse-based technology for digital data transmission with a bandwidth of 7.5 GHz. It takes a little power to operate over short distances (up to 15 m). Because of its low power spectral density (PSD) of -41.3 dBm/MHz, it may be simply and securely installed alongside current wireless communication systems without generating interference. UWB's high data rate transmission with low energy consumption and multipath resistance characteristic enables it to be used for high-accuracy wireless range in IoT applications [1].

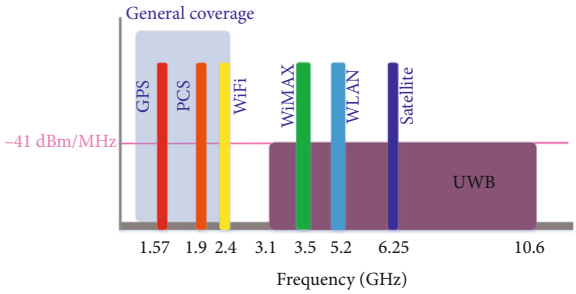

Figure 1: A comparison between the UWB spectrum and current commercial communication system spectrum [1].

On the other hand, a WSN system is a layered server architecture in which each layer is defined according to a specific function to perform. Upper and lower layers further divide network architecture into seven different layers (application, presentation, session, transport, network, data link, and physical layers). In literature, many methods and techniques have been introduced in order to minimize the energy of WSN systems. Some researches concentrated on minimizing the energy based on algorithms in the network layer [2, 3]. And other researches are interested in energy consumption at the physical layer as our work.

The wake-up receiver is an important component of wireless sensor networks. This compact receiver is used in a wide range of applications, including IoT, ambient intelligence, and personal area networks. One of the most critical difficulties in wake-up receiver design is lowering power consumption to improve battery life; Figure 2 depicts a wireless sensor node outfitted with a wake-up receiver. A detailed study on wake-up receiver and a comparison of some existing architectures have been presented in [4].

As part of its function, it is expected that the wake-up receiver can demodulate a signal, recognize in some cases a particular code, and issue a pulse to turn on the main receiver chain. As a result, its reaction time is critical since it contributes to the receiver's and the application's launch times. A communication protocol with code recognition allows the reduction of incorrect wake-up signals and so optimizes usage. Good reception is dependent on its capacity to identify undesired signals, regardless of its ability to receive weak signals or function in a variety of situations.

The signal is transmitted through an RF carrier whose frequency is an important parameter. The frequency range is chosen based on a variety of parameters. In the scenario when the wake-up receiver and the main receiver are on the same chip, it may be congruent to that of the main radio for simplicity and feature sharing. Because of space and potential coupling, we can use the same frequency to prevent intermodulation difficulties and enable the use of a single antenna. However, if no restrictions are put on the primary receiver, the use of each frequency band is governed by rules. Bluetooth, Zigbee, and other wireless technologies, for example, use the 2.4 GHz range. Working in such a band necessitates a high level of selectivity. Furthermore, the most commonly utilized band in literature [5–7] for the construction of wake-up receivers is 868 MHz; the advantage of this band, in addition to registering in the Zigbee standards, is that it is part of the ISM (Industrial Scientific Medical) band. Using this band relaxes the limits on the communication protocol, but we cannot use those wake-up receivers in UWB, wireless personal area networks (WLAN), body area networks, and other networks.

The previously described frequency band selection influences the modulation technique selection. This modulation is used to transmit data across an RF carrier. The complexity of the modulation is advantageous for signal transmission since it provides immunity when compared to other signals. The latter, on the other hand, will need more complicated circuits and is less consistent with the aim of low consumption. The first modulation approach is frequency modulation, which is difficult to execute in the context of a wake-up receiver because it is impossible to control a reference clock without employing external and active components. Furthermore, the chain design is complicated and incompatible with the goal of low consumption. The second modulation method is amplitude modulation, which has the simplest handling; it consists of multiplying an RF signal, the carrier, by an information signal, the modulating signal. The primary drawback of this modulation is the low signal-to-noise ratio (SNR) and frequency modulation. Amplitude modulation is especially well suited for passive or semipassive reception methods. In this situation, the receiver provides excellent consumption performance. There are two sorts of active reception systems that may be applied. The simplest is the chain with direct detection, which operates with no frequency change, and the more sophisticated is the chain with intermediate detection, which operates with an intermediate frequency. The most significant item in consumption in the first situation is the amplification of the RF signal, whereas the most important item in consumption in the second case is the creation of the intermediate frequency. The phase is the final signal characteristic that may be modified. This sort of modulation is commonly used in telecommunications, such as GSM and Wi-Fi. A complicated infrastructure of mixers, phase shifters, and oscillators is used to demodulate a phase-modulated signal. It is not appropriate for low-power circuits due to its complexity. We identified no realizations based on this modulation in the literature for wake-up receiver-based applications.

Among the required parameters for a wake-up receiver is sensitivity, which must be more than -70 dBm. We can overcome the low-range constraint by developing a highly sensitive receiver. The data rate is another key criterion that is primarily determined by the application, as most IoT applications require a very low rate with very occasional transfers. As a result, lower data rates can be used to reduce power consumption.

Numerous research studies on the application of the wake-up receiver have been published recently. A highly integrated and scalable 65 nm CMOS wake-up receiver was presented and manufactured in 2022 [8]. It achieves a performance of -91.5 dBm sensitivity with a power consumption of 0.9-20.9 μW for 1 s-10 ms latency. However, in [9], the authors designed only an envelope detector for the front end of a wake-up receiver. Two figures of merit to guide the optimization of the trade-offs of a MOS envelope detector

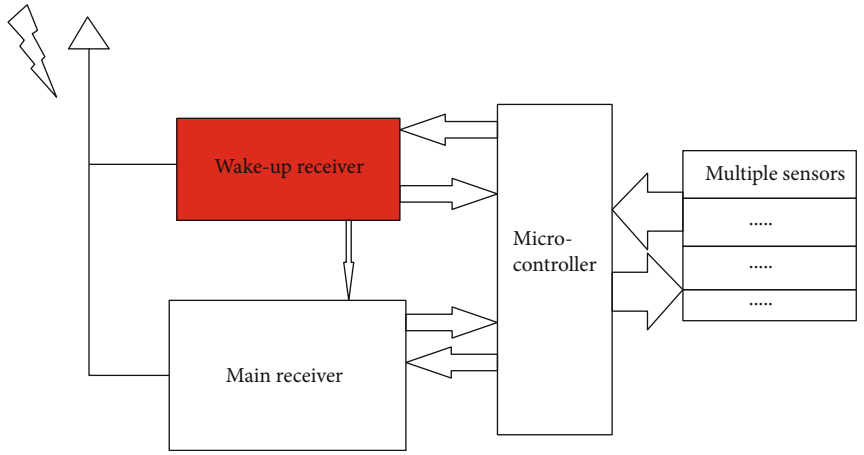

Figure 2: A wireless sensor node equipped with a wake-up receiver.

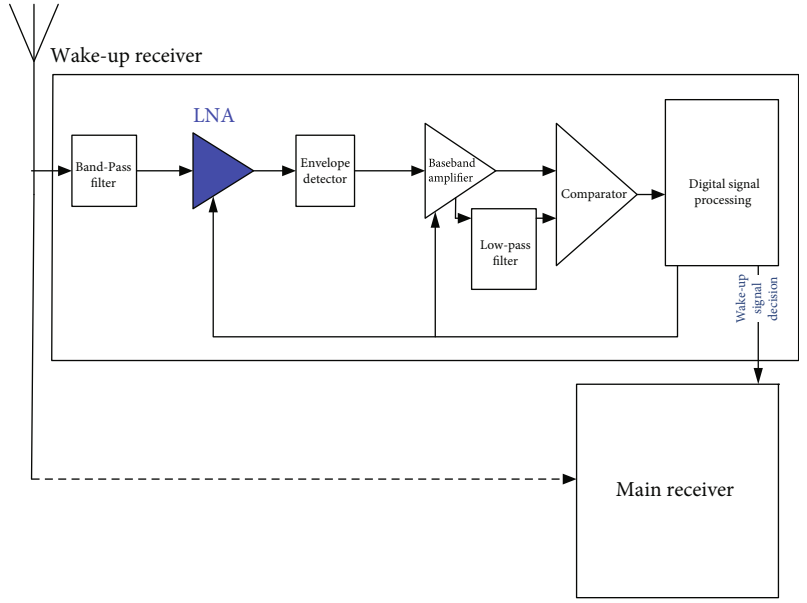

Figure 3: Wake-up receiver block diagram.

for the wake-up receiver have been presented. In [10], a novel approach for low-power WLAN mode employing a wake-up receiver is described. The suggested solution can reduce the issues that emerge when employing a duty-cycling strategy. In [11], the authors present a nanowatt-powered wake-up receiver that is made possible by a number of significant advances. Using a 130 nm CMOS technology, the wake-up receiver achieves -76 dBm at the 151.8 MHz multiuse radio service band and -71 dBm at the 433 MHz industrial, scientific, and medical band with a total DC power consumption of 7.6 nW. In [12], a mixing receiver of the LNA with back gate using a double balance mixer with doublers to merge LNA and LC-resonator quadrature voltage-controlled oscillator from balun circuit was presented. This mixing receiver implemented in the TSMC CMOS process is useful for RF systems.

On the other hand, in [13], the authors proposed a wake-up receiver based on a tuned RF architecture that requires filtering for selectivity and high RF gain for high sensitivity. This architecture fits better due to its simplicity and low cost of implementation; it consists of an LNA to amplify the received signal with minimal noise, an envelope detector to downconvert the RF signal to a baseband with a significantly lower frequency than that of the carrier, a baseband amplifier to boost the voltage level of the extracted envelope, a hysteresis comparator, and a decoder. The PIC12 is chosen for the digital part thanks to its electrical properties, internal peripherals, and space requirements. This wake-up receiver employs a modified medium access protocol that permits 3 μW of power consumption and -90 dB of detection sensitivity. In 2018, Wang et al. and Peter et al. suggested three distinct wake-up receivers [14–16], whose essential design includes a transformer filter, an envelope detector, a comparator, and a digital baseband. In accordance with [14], they use an active envelope detector, and this study presents a 113.5 MHz OOK-modulated wake-up receiver that

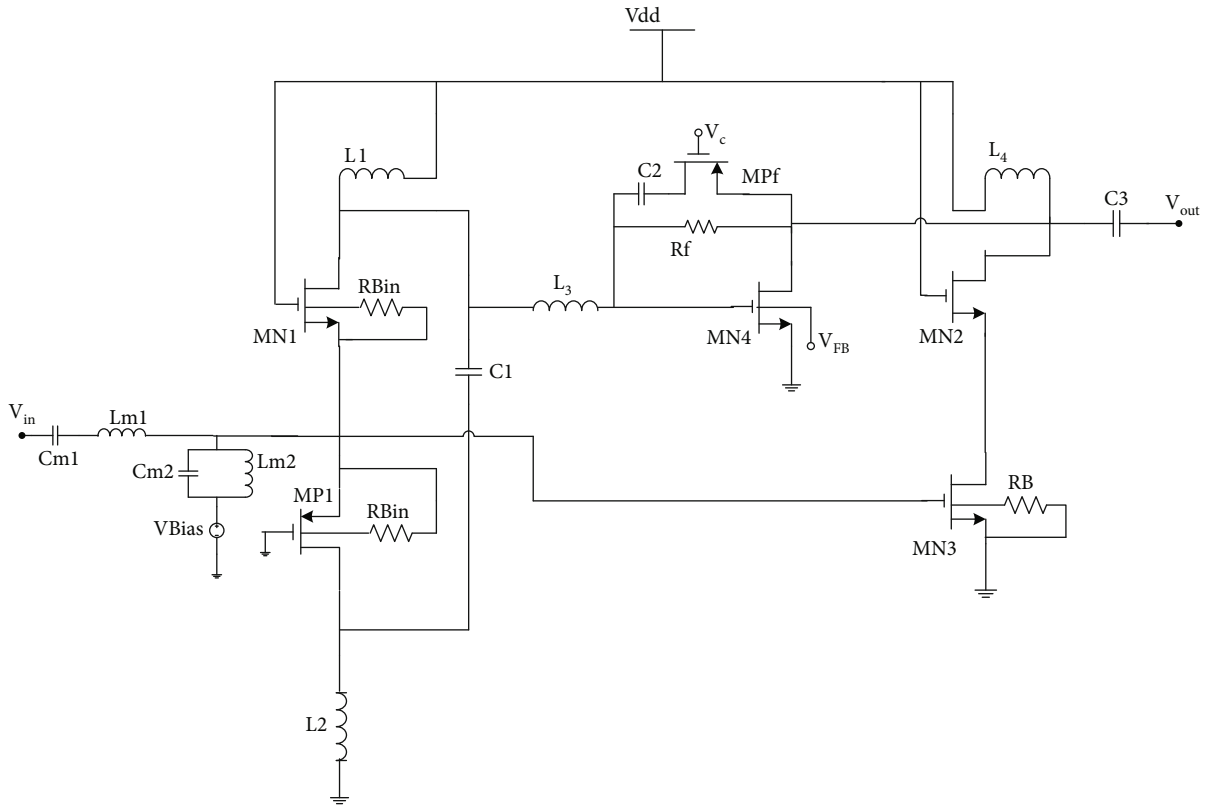

Figure 4: Schematic of the proposed LNA.

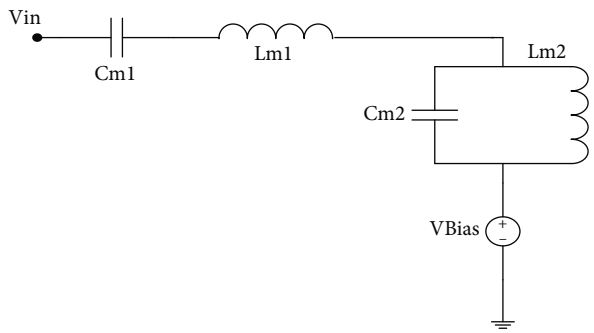

Figure 5: The used Chebyshev filter.

achieves -69 dB sensitivity while consuming just 4.5 mW of power. Using a passive pseudobalun envelope detector with an LNA, the authors of [15] obtain a sensitivity of -80.5 dBm with just 6.1 nW. Therefore, active envelope detector systems can achieve ultralow power operation, but with limited sensitivity in the absence of substantial RF voltage gain and low-noise baseband circuitry. Using an active pseudobalun envelope detector, Peter et al. [16] accomplish a 400 MHz, 4.5 nW power, and -63.8 dB sensitivity wake-up receiver using this approach. All preceding systems employ the same digital baseband, which is a correlator that analyzes incoming data by calculating the hamming distance between the sequence and the programmable oversampling code. Once the value falls below a certain threshold, the detected pattern is declared and the correlator generates a wake-up signal. Almost all of the previously described wake-up receiver designs operate in a low-frequency spectrum, with some also operating in the 2.4 GHz frequency.

As part of other designs and implementation of the WLAN wake-up receiver, we focus on the design of a low-power LNA using RF-TSMC CMOS 0.18 μm technology. The LNA is an important block in the receiver chain, since it significantly increases the receiver sensitivity, and its performance is a challenge for RF circuit designers. As the LNA is the first component in the signal reception chain that receives the signal after the antenna, any noise created by this amplifier will be carried throughout this chain, affecting the performance of subsequent components; therefore, it is vital to take this parameter into account. As depicted in Figure 3, the LNA amplifier is used to amplify the signal received from the antenna without adding noise. In the case of long-distance communication, such as satellite communication, where waves are transmitted over unguided propagation lines tens or hundreds of kilometers long, the front components must meet the strict requirements that a good link between the different agents of each link requires. In this case, the front-end transistors of the amplifier must be able to meet these requirements. In addition, several research studies focusing only on the LNA's implementation have been published [17–21].

The rest of the paper is organized as follows: in Section 2, low-noise amplifier design is discussed. The S-parameters, harmonic balance, and Monte Carlo and PVT simulation results of the designed circuits are presented in Section 3. Section 4 concludes the paper.

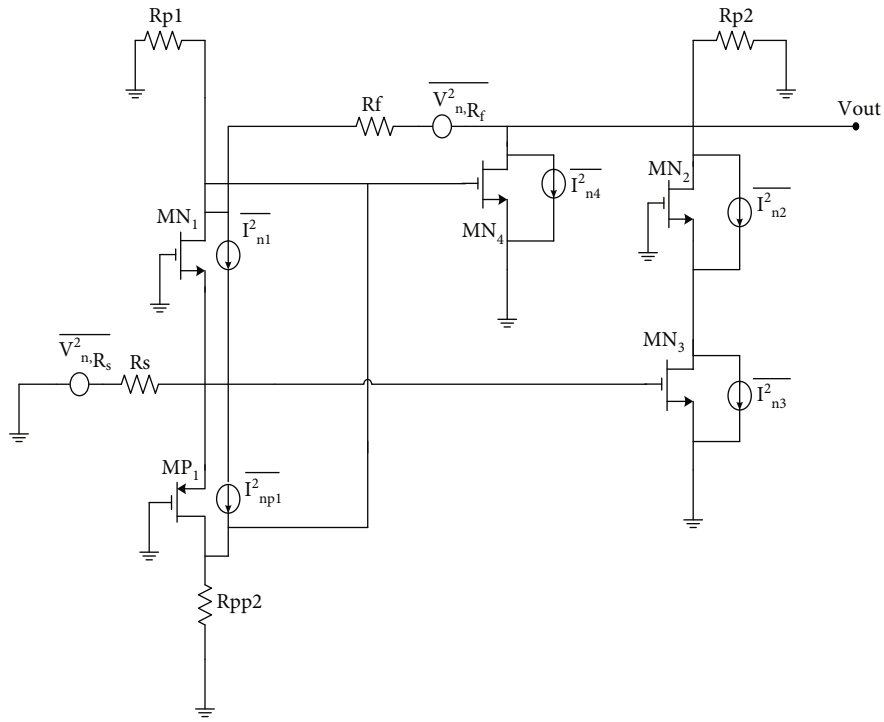

Figure 6: The designed LNA equivalent circuit.

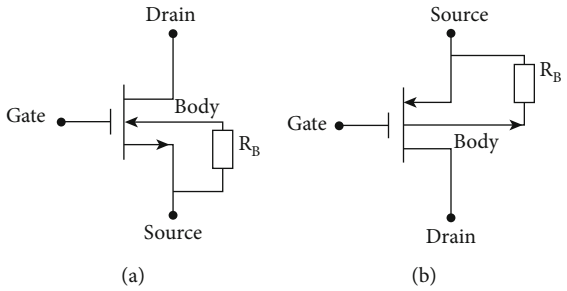

Figure 7: MOS schematic with larger substrate R_B. (a) Schematic of NMOS with R_B. (b) Schematic of PMOS with R_B.

2. Methods

2.1. LNA Implementation. Figure 4 illustrates the topology of the proposed LNA. It consists of two stages with resistive shunt-shunt feedback. The common-gate topologies MN_1 and MP_1 are positioned as the input stage in order to decrease power consumption and generate a broad input match throughout the frequency range of interest. Due to the trade-off between input matching and gain in the common-gate stage, a common-source stage MN_4 is added to achieve high gain. A shunt-shunt feedback structure is used to adjust the gain by changing the feedback resistance, providing a gain that is continuously varied. V_c is connected to the gate of MP_f, and no further driving current is necessary.

By utilizing inductors $L_1, L_2,$ and L_3 as shunt inductive peaking and series inductive peaking, respectively, the bandwidth of interest is increased. The capacitances $C_1, C_2, C_3,$ and C_4 are employed for DC bias isolation.

The input stage is formed of the MN_1 and MP_1 transistors. Consequently, the MN_2 and MN_3 transistors are used to minimize the main noise source, MN_1. Recognizing that each transistor has a unique noise figure, we used $R_{B\text{in}}$ and R_B resistors to reduce the noise figure of each transistor, hence lowering the noise figure of the entire circuit.

2.2. Input Matching. The Chebyshev filter has the benefit of a sharp roll in the factor stop band and ripples in the pass band. This filter resonates the input impedance reactive portion across the operational frequency range. Numerous studies utilizing a Chebyshev filter in the LNA implementation design have been published. In [22], a simple Chebyshev filter is used to match the input bandwidth. This input network is less complicated and has an excellent reflected coefficient between 3.1 GHz and 10.6 GHz. As the input stage in [23], a Chebyshev filter has been built with the goal of providing the appropriate higher-end and lower-end cutoff frequencies.

In addition, a Chebyshev filter was employed in [24] to get wideband input matching and flat gain. Figure 5 depicts the used filter.

2.3. Low-Voltage Technique Analysis. Forward body biasing is applied to reduce the transistor's the T is a V index voltage. The lowering of the T is a V index enables low the DD is a V index operation and enhances circuit design freedom. According to the simulation, the MN_4 transistor consumes the most power; thus, forward body biasing will be applied to this transistor.

V_T of NMOS can be expressed as follows:

$$V_T = V_{T0} + \gamma\left[\sqrt{2\Phi_f + V_{SB}} - \sqrt{2\Phi_f}\right], \quad (1)$$

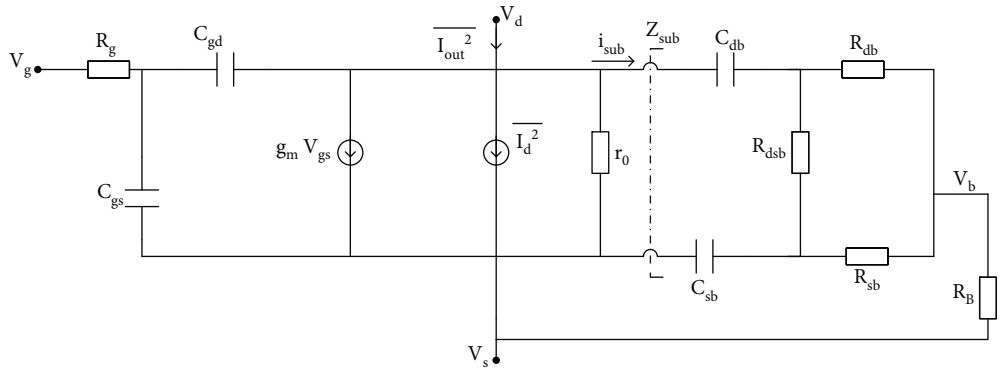

Figure 8: Noise equivalent circuit of a MOS device with R_B.

Table 1: Inductor optimized values.

Inductor	Optimized value (nH)
L_1	3
L_2	2
L_3	4
L_4	3

Table 2: Capacitor optimized values.

Capacitor	Optimized value (pF)
C_1	1.5
C_2	1
C_3	3

Table 3: Transistor parameters.

Transistor	Finger × W (μm) × L (μm)
MN_1	24 × 3.6 × 0.18
MP_1	50 × 4.6 × 0.18
MN_2	21 × 1 × 0.18
MN_3	14 × 1 × 0.18
MN_4	10 × 7.7 × 0.18
MP_f	25 × 1.4 × 0.18

where V_{T0} is the threshold voltage with zero-body-source voltage, γ is the body effect coefficient, and Φ_f is the bulk Fermi potential. In this brief, the voltage between the body and the source of the transistor MN_4 is biased reversely $V_{SB} < 0$ V for reducing V_T. According to the simulation, The T is a V index of an NMOS transistor can be lowered to 0.38 V when the body-to-source voltage V_{BS} is equal to 0.45 V. As a result, the supply voltage and power consumption are reduced.

2.4. Noise-Reduction Technique Analysis. To analyze the noise figure of the designed LNA depicted in Figure 4, the noise equivalent circuit without R_B and R_{Bin} consideration is shown in Figure 6.

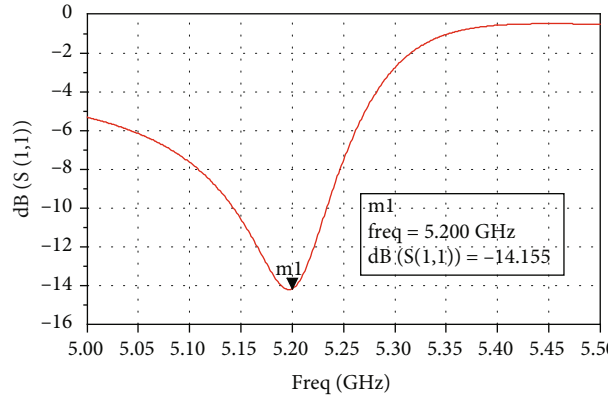

Figure 9: Simulated input reflection coefficient S21.

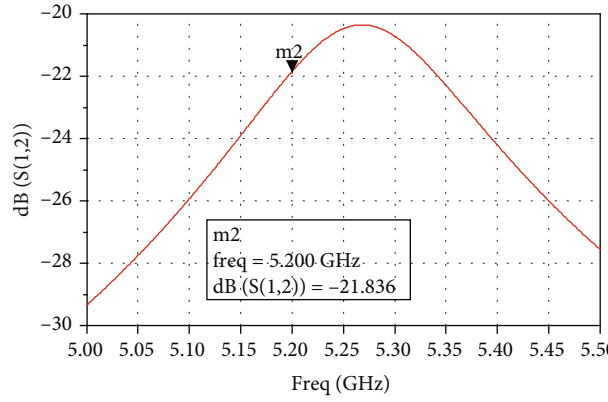

Figure 10: Reverse isolation S12.

The designed LNA total noise figure is given as follows:

$$\mathrm{NF}_{\mathrm{tot}} = 1 + \frac{\left(g_{\mathrm{mn4}}R_{\mathrm{peq}}\right)^2 \gamma/\alpha\left(g_{\mathrm{mn1}} + g_{\mathrm{mp1}}\right)}{R_s\left(g_{\mathrm{mn4}}R_{\mathrm{peq}}\left(g_{\mathrm{mn1}} + g_{\mathrm{mp1}}\right) + g_{\mathrm{mn3}}\right)^2} + \frac{\left(1 + \left(\left(g_{\mathrm{mn1}} + g_{\mathrm{mp1}}\right)R_s\right)^2\left(\gamma/\alpha(g_{\mathrm{mn3}} + g_{\mathrm{mn4}}) + R_f\right)\right)}{R_s\left(g_{\mathrm{mn4}}R_{\mathrm{peq}}\left(g_{\mathrm{mn1}} + g_{\mathrm{mp1}}\right) + g_{\mathrm{mn3}}\right)^2}. \quad (2)$$

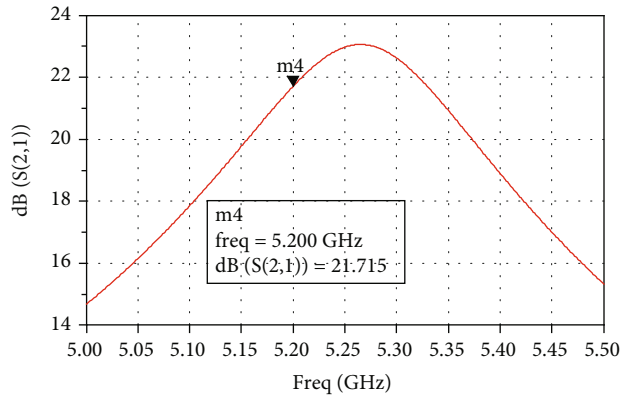

Figure 11: Simulated power gain.

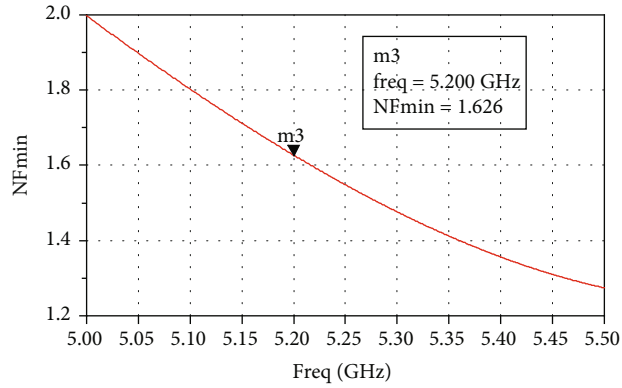

Figure 12: Noise figure simulation result.

We may assume that, with the exception of MP_f and MN_2, all transistors have an influence on the overall noise figure; thus, we want to minimize the noise figure of each concerned transistor in order to reduce the total noise figure.

R_B is a substrate resistor that may be used to minimize noise in a MOS device and hence improve the noise performance of the LNA.

Figure 7 depicts a schematic of MOS transistors with a substrate resistance R_B. The noise equivalent circuit of a MOS device with substrate resistance R_B is shown in Figure 8.

Generally, the substrate impedance Z_{sub} can be simplified to a simple series RC circuit as follows:

$$Z_{\text{sub}} \cong \frac{1}{j\omega C_{db}} + \frac{R_{db}(R_{sb} + R_{dsb})}{R_{db} + R_{sb} + R_{dsb}} + R_B. \tag{3}$$

So, the substrate resistance R_{sub} is expressed as follows:

$$R_{\text{sub}} = \frac{R_{db}(R_{sb} + R_{dsb})}{R_{db} + R_{sb} + R_{dsb}} + R_B. \tag{4}$$

The noise figure NF can be expressed as [25]

$$\text{NF} = \text{NF}_{\text{min}} + \frac{G_n}{R_s}\left(Z_s - R_{\text{opt}} - jX_{\text{opt}}\right)^2. \tag{5}$$

The minimum noise figure NF_{min} and the noise parameter G_n can be written as

$$\text{NF}_{\text{min}} = 1 + 2G_n\left(R_g + R_s + R_{\text{opt}}\right), \tag{6}$$

$$G_n = \left[\frac{K_g(\omega)^2 C'^2{}_{gs}}{g_m} * \left(1 + \frac{R_d}{R_{ds} \| R_{\text{sub}}}\right)\right]. \tag{7}$$

From Equation (3), adding a substrate resistor R_B increases the substrate impedance Z_{sub}. According to Equations (6) and (7), increasing the equivalent substrate resistor R_{sub} decreases the minimal noise figure NF_{min}; moreover, decreasing NF_{min} and G_n reduces the noise figure NF in Equation (5).

2.5. Gain Control Circuit. The gain control structure is depicted in Figure 4 at the second stage. We can change the gain by adjusting V_c, the bias voltage. It should be noted that V_c is placed at the gate of MP_f and may be written as

$$R_{\text{on}} = \frac{1}{\mu_p C_{\text{ox}}(W/L)_f (V_C - V_{th})}. \tag{8}$$

Taking into account that MP_f is a PMOS transistor and according to Equation (8), the transimpedance gain is controlled by decreasing V_c.

3. Simulation Results

3.1. S-Parameter Simulation Results. Using ADS, the suggested LNA is developed and simulated in the RF-TSMC CMOS 0.18 μm technology. We applied the existing ADS optimization algorithm. We may establish our targets, the type of optimization, and eventually the range of the required optimized parameters using this approach. The circuit uses 1.45 mW of direct current electricity and has a supply voltage of 0.6 volts. The circuit is optimized with the primary objective of reducing noise, giving a high gain and good input matching, and retaining acceptable circuit parameter values in consideration.

Table 1 shows the optimized inductor values, whereas Table 2 shows the optimal capacitance values. It should be noted that the inductance and capacitance values should be as low as feasible in order to be implemented.

The transistor LNA's needed design characteristics are shown in Table 3. By selecting a minimum transistor length of 0.18 μm, the LNA's bandwidth is raised and the parasitic capacitors are minimized.

The S-parameter analysis is carried out between 5 and 6 GHz. For the remainder of the simulations, we will concentrate on the results at 5.2 GHz, since the ISM band specification for the IEEE 802.11a in the WLAN standard was adopted for the carrier frequency 5.2 GHz, as shown in Figure 1. Due to the requirement for a greater transmission rate, 802.11b with 11 Mbit/s is clearly inferior to 802.11a, which is a modification to the IEEE 802.11 protocol that adds a higher data rate of up to 54 Mbit/s utilizing the 5.2 GHz band [19].

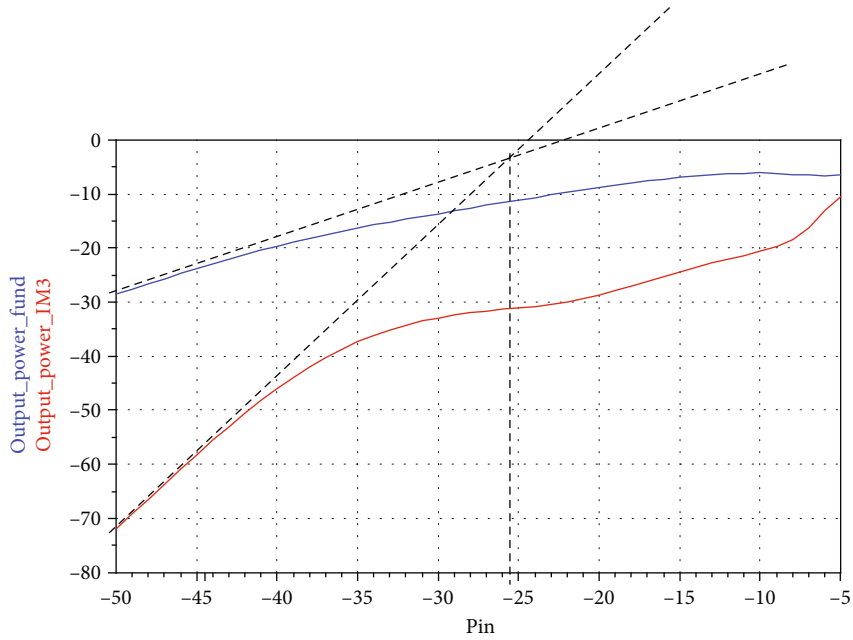

Figure 13: Simulated IIP3 of the proposed circuit.

Table 4: Comparison to previous work simulation results.

Reference	[17]	[18]	[19]	[27]	This work
Tech	ATF21xx	0.18 μm	0.18 μm	65 nm	0.18 μm
F (GHz)	5.2	5.2	5.2	5.2	5.2
G_{max} (dB)	11.3	16	12.96	15.5	21.7
NF_{min} (dB)	0.78	2.5	1.0	2.2	1.6
V_{dd} (V)	4	1.8	1.8	1.2	0.6
Power (mW)	50	4.5	—	7.7	0.87
S11 (dB)	-17	-30	-50.4	-10.3	-14.15
IIP3 (dBm)	27.8	—	—	-9.3	-26.5
FoM	-1.02	2.37	—	1.677	41.57

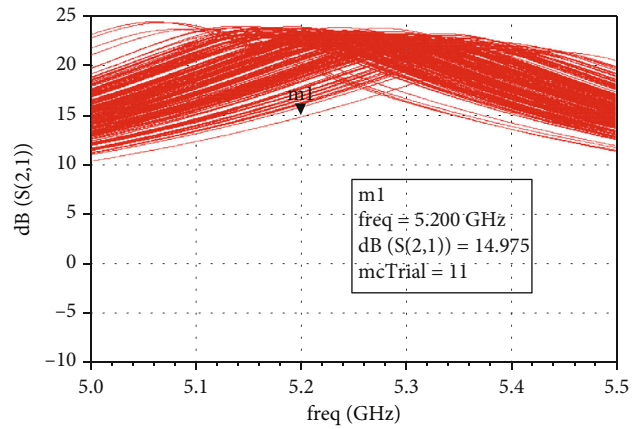

Figure 14: S21 Monte Carlo simulation.

The simulated input reflection coefficient S11 is shown in Figure 9. S11 equals -14.15 dB at 5.2 GHz.

The reverse isolation is shown in Figure 10. At 5.2 GHz, the S-parameter coefficient S12 is smaller than -21.8 dB. The gain power is equal to 21.7 dB at 5.2 GHz, which is illustrated in Figure 11.

Figure 12 illustrates the simulation results for the noise figure. The proposed LNA exhibits a minimum noise figure of roughly 1.6 dB at 5.2 GHz.

The S-parameter simulations of the proposed LNA are shown in Figures 9–12. Based on this analysis, we may conclude that the suggested design presents better performances than several existing circuits in the literature.

3.2. Harmonic Balance Simulation Result. We used the harmonic balance simulation to validate the designed LNA. To calculate intermodulation distortion products and third-order interception point, two-input tones of the same strength but separated by a very short frequency offset or spacing can be employed. At various mixing frequencies, these two tones combine and produce higher-order distortion products.

As seen in Figure 13, the value of the IIP3 point is equal to -26.5 dBm which represents a good linearity for such a nonlinear device.

To compare the performances of the LNAs, the figure of merit (FoM) is calculated as defined in [26]:

$$\text{FoM} = \frac{\text{Gain}}{(\text{NF} - 1) * P_{\text{dc}}}. \quad (9)$$

Table 4 compares the proposed LNA's circuit performance to that of various earlier published researches.

3.3. Monte Carlo Simulation. A series of Monte Carlo simulations were done to demonstrate the impact of process

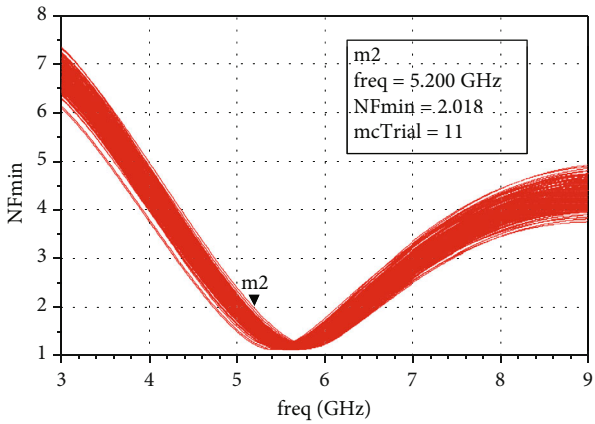

Figure 15: Noise figure Monte Carlo simulation.

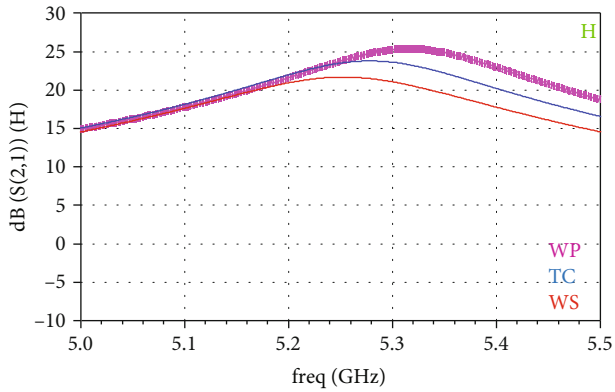

Figure 16: S21 PT simulation.

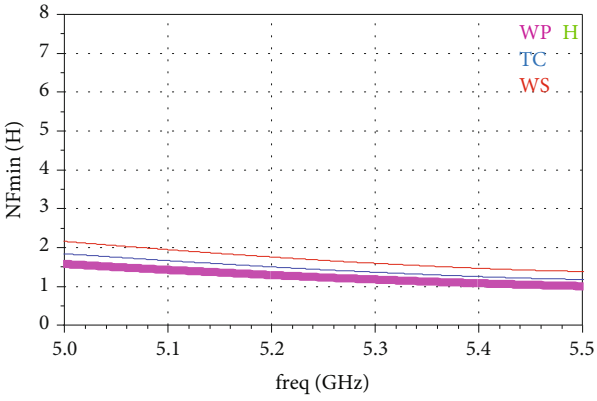

Figure 17: Noise figure PT simulation.

modifications on the performance parameters of the LNA. The Monte Carlo analysis was used to reduce the size of all circuit transistors by 5%.

Figures 14 and 15 show the results of the Monte Carlo analysis. The gain parameter of the LNA is shown in Figure 14, which is more than 14.9 dB for 200 Monte Carlo simulation runs at 5.2 GHz. The noise figure parameter of the LNA is less than 2 dB for 200 Monte Carlo simulation runs in the same frequency range, as shown in Figure 15.

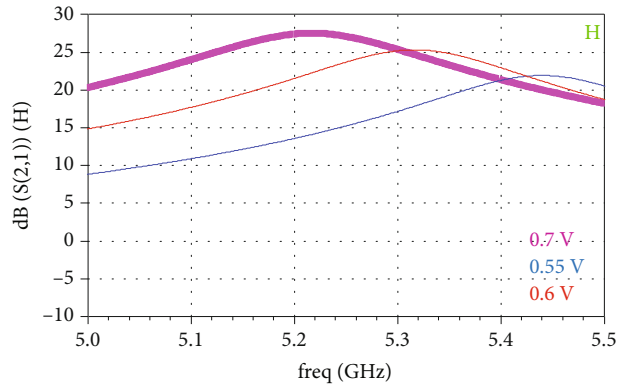

Figure 18: S21 simulations for different supply voltages.

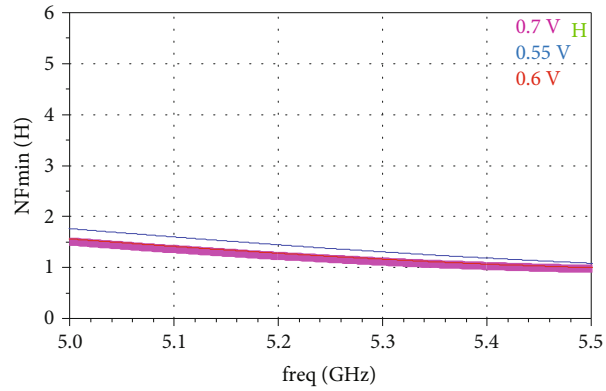

Figure 19: Noise figure simulations for different supply voltages.

3.4. PVT Simulation. The performance of this LNA was evaluated at various process corners, supply voltages, and temperatures to assess its sensitivity to PVT variations. Gain and noise figure are the factors evaluated for PVT adjustments. The process corners used in this simulation were given by the foundry.

First, three cases were considered: the first (TC) is the most typical case, in which all of the transistors have a typical model and the circuit operates at 0°C. The second case (WP) considers operating circumstances where the temperature is -45°C and the models of all transistors conform to the FF (fast-fast) model. The transistors in the third case (WS) employ the SS (slow-slow) model, and the temperature is around 50°C.

At 5.2 GHz, the PT (Process-Temperature) change has no influence on the power gain value, as illustrated in Figure 16. While temperature has little influence on the noise figure value (Figure 17), it is still less than 2 dB for different temperatures.

Knowing that lowering the supply voltage is a way used in this article to minimize power usage, the values examined were 0.7 V, 0.6 V, and 0.55 V.

As shown in Figure 18, at 5.2 GHz, the supply voltage variation has little effect on the power gain value, but the minimum gain value is about 21 dB. However, the supply voltage variation has no effect on the noise figure value (Figure 19).

4. Conclusion and Future Works

The presented work describes a low-power WLAN LNA for WSN wake-up receiver applications. The system is designed to give more importance to the reduction of power consumption and noise figure. Implemented in a 0.18 μm CMOS technology, the suggested LNA consumes 0.87 mW. The maximum gain attained at 5.2 GHz is approximately 21.7 dB. The minimum noise level is around 1.6 dB as a high substrate resistance is used to reduce the noise figure. Corner simulations are done to observe the circuit's immunity to PVT changes as well as Monte Carlo simulations to prove the performance of the LNA. It can be concluded from the analysis that our design has presented advantages in almost all performance parameters. Hence, the circuit is suitable for applications which need low power consumption, low noise, and low-cost solution for WSN wake-up receivers. In future work, we intend to develop the entire WLAN wake-up receiver architecture for WSN applications.

Data Availability

The data used to support the findings of this study are available from the corresponding author upon request.

Disclosure

This work is under a PhD project which is not financed.

Conflicts of Interest

The authors declare that they have no conflicts of interest.

References

[1] L. Wang, Y. Xiong, and M. He, "Review on UWB bandpass filters," in *UWB Technology-Circuits and Systems*, IntechOpen, London, United Kingdom, 2019.

[2] S. Dutt, N. J. Ahuja, and M. Kumar, "An intelligent tutoring system architecture based on fuzzy neural network (FNN) for special education of learning disabled learners," *Education and Information Technologies*, vol. 27, no. 2, pp. 2613–2633, 2022.

[3] P. Chithaluru, F. Al-Turjman, M. Kumar, and T. Stephan, "MTCEE-LLN: multilayer threshold cluster-based energy-efficient low-power and lossy networks for Industrial Internet of Things," *IEEE Internet of Things Journal*, vol. 9, no. 7, pp. 4940–4948, 2022.

[4] M. Bouraoui, I. Barraj, and M. Masmoudi, "Study on wake-up receiver design for IoT applications," in *2019 IEEE International Conference on Design & Test of Integrated Micro & Nano-Systems*, pp. 1–4, Gammarth, Tunisia, 2019.

[5] S. Bdiri, F. Derbel, and O. Kanoun, "An 868 MHz 7.5 μW wake-up receiver with −60 dBm sensitivity," *Journal of Sensors and Sensor Systems*, vol. 5, no. 2, pp. 433–446, 2016.

[6] H. Milosiu, F. Oehler, M. Eppel et al., "A 3-μW 868-MHz wake-up receiver with −83 dBm sensitivity and scalable data rate," in *2013 Proceedings of the ESSCIRC (ESSCIRC)*, pp. 387–390, Bucharest, Romania, 2013.

[7] F. A. Aoudia, M. Gautier, and O. Berder, "OPWUM: opportunistic MAC protocol leveraging wake-up receivers in WSNs," *Journal of Sensors*, vol. 2016, Article ID 6263719, 9 pages, 2016.

[8] R. Ma, F. Protze, and F. Ellinger, "A 193-nW wake-up receiver achieving −84.5-dBm sensitivity for green wireless communications," *IEEE Transactions on Green Communications and Networking*, vol. 6, no. 1, pp. 512–529, 2022.

[9] A. Dissanayake, H. L. Bishop, S. M. Bowers, and B. H. Calhoun, "A 2.4 GHz-91.5 dBm sensitivity within-packet duty-cycled wake-up receiver," *IEEE Journal of Solid-State Circuits*, vol. 57, no. 3, pp. 917–931, 2022.

[10] J. Blobel, F. Menne, D. Yu, X. Cheng, and F. Dressler, "Low-power and low-delay WLAN using wake-up receivers," *IEEE Transactions on Mobile Computing*, vol. 21, no. 5, pp. 1739–1750, 2022.

[11] L. Reyes and F. Silveira, "Gain, signal-to-noise ratio and power optimization of envelope detector for ultra-low-power wake-up receiver," *IEEE Transactions on Circuits and Systems II: Express Briefs*, vol. 66, no. 10, pp. 1703–1707, 2019.

[12] W.-C. Lai, "Mixing wake-up receiver of low noise amplifier with back-gated QVCO," in *2021 International Conference on Electrical, Computer and Energy Technologies (ICECET)*, pp. 1–4, Cape Town, South Africa, 2021.

[13] S. Bdiri, F. Derbel, and O. Kanoun, "A tuned-RF duty-cycled wake-up receiver with −90 dBm sensitivity," *Sensors*, vol. 18, no. 2, p. 86, 2018.

[14] P.-H. P. Wang, H. Jiang, L. Gao et al., "A near-zero-power wake-up receiver achieving −69-dBm sensitivity," *IEEE Journal of Solid-State Circuits*, vol. 53, no. 6, pp. 1640–1652, 2018.

[15] P.-H. P. Wang, H. Jiang, L. Gao et al., "A 6.1-nW wake-up receiver achieving −80.5-dBm sensitivity via a passive pseudo-balun envelope detector," *IEEE Solid-State Circuits Letters*, vol. 1, no. 5, pp. 134–137, 2018.

[16] W. P. Peter, J. Haowei, G. Li et al., "A 400MHz 4.5nW -63.8 dBm sensitivity wake-up receiver employing an active pseudo-balun envelope detector," in *43rd IEEE European Solid-State Circuits Conference*, pp. 35–38, Leuven, Belgium, 2017.

[17] M. El Bakkali, N. AmarTouhami, H. ElFtouh, and A. Marroun, "Design of 5.2 GHz low noise amplifier for wireless LAN," *Procedia Manufacturing*, vol. 32, pp. 739–744, 2019.

[18] V. K. Dao, B. G. Choi, and C. S. Park, "Dual-band LNA for 2.4/5.2GHz applications," in *2006 Asia-Pacific Microwave Conference*, pp. 413–416, Yokohama, Japan, 2006.

[19] H. C. Yang, S. H. Peng, S. J. Wang et al., "High quality of 0.18μm CMOS 5.2GHz cascode LNA for RFID tag applications," in *2013 International Symposium on Next-Generation Electronics*, pp. 313–316, Kaohsiung, Taiwan, 2013.

[20] Hemad Heidari Jobaneh, "The design of an ultralow-power ultra-wideband (5 GHz–10 GHz) low noise amplifier in 0.13 μm CMOS technology," *Active and Passive Electronic Components*, vol. 2020, Article ID 8537405, 12 pages, 2020.

[21] M. Bouraoui, I. Barraj, A. Neifar, and M. Masmoudi, "An ultra-wideband noise-reduction LNA with variable gain for wireless wake-up receivers," in *2022 IEEE International Conference on Design & Test of Integrated Micro & Nano-Systems (DTS)*, pp. 01–05, Cairo, Egypt, 2022.

[22] B.-Y. Chang and C. F. Jou, "Design of a 3.1-10.6GHz low-voltage, low-power CMOS low-noise amplifier for ultra-wideband receivers," in *2005 Asia-Pacific Microwave Conference Proceedings*, Suzhou, China, 2005.

[23] A. P. Tarighat and M. Yargholi, "Linearized low noise amplifier by post distortion technique," in *2019 27th Iranian Conference on Electrical Engineering (ICEE)*, pp. 205–208, Yazd, Iran, 2019.

[24] N. Gautam, M. Kumar, and A. Chaturvedi, "A 3.1-10.6 GHz CMOS two stage cascade topology low-noise amplifier for UWB system," in *2014 Fourth International Conference on Communication Systems and Network Technologies*, pp. 1070–1073, Bhopal, India, 2014.

[25] K. Chen and S. I. Liu, "Inductorless wideband CMOS low-noise amplifiers using noise-canceling technique," *IEEE Transactions on Circuits and Systems I: Regular Papers*, vol. 59, no. 2, pp. 305–314, 2012.

[26] A. Taibi, A. Slimane, M. T. Belaroussi, S. A. Tedjini, and M. Trabelsi, "Low power and high linear reconfigurable CMOS LNA for multi-standard wireless applications," in *2013 25th International Conference on Microelectronics (ICM)*, pp. 1–4, Beirut, Lebanon, 2013.

[27] D. M. Kim, E. Yang, and D. Im, "A concurrent dual-band CMOS partial feedback LNA with noise and input impedance matching optimization for advanced WLAN applications," *Journal of Semiconductor Technology and Science*, vol. 21, no. 5, pp. 356–363, 2021.

Hindawi
Journal of Sensors
Volume 2022, Article ID 8244176, 8 pages
https://doi.org/10.1155/2022/8244176

Research Article

A Novel Routing Protocol for Low-Energy Wireless Sensor Networks

Sebastin Suresh,[1] V. Prabhu,[2] V. Parthasarathy,[3] Rajasekhar Boddu,[4] Yadala Sucharitha,[5] and Gemmachis Teshite[4]

[1]*Anna University, Chennai, India*
[2]*Vel Tech Multi Tech Dr. Rangarajan Dr. Sakunthala Engineering College, Chennai, India*
[3]*Karpagam Academy of Higher Education, Coimbatore, India*
[4]*Department of Software Engineering, College of Computing and Informatics, Haramaya University, Dire Dawa, Ethiopia*
[5]*Department of Computer Science and Engineering, CMR Institute of Technology, Hyderabad, TS State, India*

Correspondence should be addressed to Rajasekhar Boddu; rajsekhar.boddu@haramaya.edu.et

Received 15 June 2022; Revised 29 July 2022; Accepted 9 August 2022; Published 27 August 2022

Academic Editor: Eunsung Oh

The battery power limits the energy consumption of wireless sensor networks (WSN). As a result, its network performance suffered significantly. Therefore, this paper proposes an opportunistic energy-efficient routing protocol (OEERP) algorithm for reducing network energy consumption. It provides accurate target location detection, energy efficiency, and network lifespan extension. It is intended to schedule idle nodes into a sleep state, thereby optimising network energy consumption. Sleep is dynamically adjusted based on the network's residual energy (RE) and flow rate (FR). It saves energy for a longer period. The sleep nodes are triggered to wake up after a certain time interval. The simulation results show that the proposed OEERP algorithm outperforms existing state-of-the-art algorithms in terms of accuracy, energy efficiency, and network lifetime extension.

1. Introduction

WSNs are framed by sensor combinations used for monitoring various environmental parameters. These nodes required a high energy consumption to transmit data [1]. The integration of battery power supply has improved the performance of WSNs. However, due to the limited battery life, many WSNs are prone to energy depletion. Most of the protocols do not focus on the energy distribution of the nodes [2]. This means that the routes chosen for energy consumption can only be used for specific applications. The main reason for packet loss is due to the improper network partition [3] and the retransmission of a packet consuming more energy [4]. WSNs advance in terms of raw data generation volume [5]. However, radio spectrum scarcity and the strain on resource management increase tenfold [6]. Researchers have been working on a clustering method that can better utilise valuable radio spectrum for several years. The sensed data can be transmitted to the node's licenced spectrum status of primary devices and reused within interference constraints. In [7], it describes WSNs that use cognitive radios for spectrum sensing, spectrum access, and interference management. Improve network energy efficiency by taking into account the minimum data rate and interference limits in CR-based WSNs [8] in order to maintain maximum EE in networks with energy-constrained devices (e.g., sensors, actuators, and controllers). Device-to-device (D2D) communication has been widely used in IoT networks to reduce transmission delays and power consumption while also improving spectrum efficiency [9]. Under interference constraints, two nodes can communicate directly with each other using the same radio resource of cellular devices

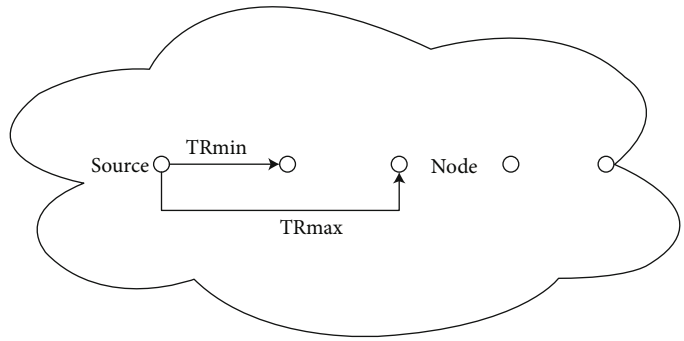

Figure 1: Basic 1-dimensional WSN.

[10]. However, strict latency and reliability requirements necessitated resource management approaches proposed in works [11–14].

1.1. Sensor Node Functions in Networking. A wide range of tasks are carried out by sensor nodes, which are widely dispersed throughout a sensitive environment. These include transmission and reception, sensing, and location tracking (GPS), processing and storing data, sleeping and communication modes, and calculation modes.

1.1.1. Transmitter/Receiver Function. The function is transmitting and receiving data from the target, which is communication between the nodes to the sink/base station.

1.1.2. Sensing Operation. The sensing operation is emitting the EM waves, and the received radio signals are used for tracking the targets.

1.1.3. Global Positing System. GPS is used for finding the position and finding the other node information in the network.

1.1.4. Data Processing. The data processing will process a received data and calculate the target location. The result of data processing is transmitted to data storage.

1.1.5. Data Storage. This function will store the data from the receiver data and the processing data.

1.1.6. The Battery. The battery will play the major role in giving energy to the senor nodes to do all the processes.

1.1.7. Sleeping Mode. Sleep mode will reduce the energy consumption of the sensor nodes, and it will increase the network lifetime.

1.1.8. Sensing Mode. This mode will sense the information about the target location; it is used to find the location of the target.

1.1.9. Listening Function. The listening function observes the senor node results.

1.1.10. Communication Operation. In the communication operation, the sensor node transmits and receives the sensed data by the sensor nodes.

1.1.11. Calculating Mode. In the calculating mode, the sensed data processed the data into the target.

2. Related Work

Relay nodes would transmit the packet size using a convention of a routing method to reduce energy consumption and hop counts [15]. Figure 1 shows the 1-dimesional WSN for data transmission. The EXOR method is a new approach to controlling packet forwarding and reducing the number of packets in transmissions. For forwarding, nodes no longer need to be scheduled at random in this new method. Geographic Random Forwarding (GeRaf) will not focus on the energy consumption of the network but instead will select a good relay node between the forwarding multiple nodes. As the forwarder set is selected, an energy-efficient opportunistic routing scheme is proposed for the network, which puts nodes into sleep mode [16]. For energy savings, the SMAC method uses the MAC layer to select random nodes and turn them into sleep nodes, forming a sleeping schedule with their nearby nodes [17]. It allows for an equal distribution of nodes, but not for energy consumption. In a random sleep schedule system, the node is put into sleep mode. Network energy dissipation can be achieved by selecting a sleep schedule that is based on the distance of each hop. TDMA scheduling and an asynchronous duty cycling system can be used to avoid idle node energy consumption by using uneven clustering to improve energy efficiency [18]. The nodes are constantly awakened by the synchronous protocol for the specified period. The sleeping node is awakened by pressing the trigger, allowing the transmission to begin. There are numerous applications for wireless sensor networks, including collecting and obtaining data from sensors, as well as effectively processing the data [19]. Battery-powered sensors are used in the network because they require a power supply to operate. When the batteries run out, the wireless sensor network will no longer function properly [20]. Due to these difficulties, changing a sensor node's battery only requires a few controlled settings, which have been discussed in many studies. The sensor nodes have limited energy ranges to extend the network's lifespan [21].

Based on WSNS surveillance issues [22–24, 33] to reduce energy consumption and at the same time improve location detection, multiple grids can be used. In [25–27, 34], the genetic algorithm was improved by using fewer sensor

Step 1. Install the node into a network
(Input parameter: optima distance and threshold energy
Output parameter: sleep/awake scheduling)
Step 2. Check the optima distance and threshold energy
Step 3. Set the flow rate
Step 4. Calculate the priority node value
Step 5. Check the entire FS (K) node for priority
Step 6. Put to sleep the high-priority node
Step 7. Calculate the sleep interval time to sleep
Step 8. Wake up the node after the sleep interval
Step 9. Start the data relaying process

Algorithm 1: Steps for OEERP Algorithm

Table 1: Simulation parameters.

Parameter (value)
Distance between two neighboring nodes (5 to 25 m)
Deployment (uniform distribution)
Sending rate (1 packet/s)
Packet size (1024 bits)
Number of nodes (100)
Source node (1)
Sink node (1)

nodes, full-area coverage, energy efficiency, and connectivity controlled by a sensor order. WSNs can benefit from a fuzzy data fusion method [28]. The sensor node used more energy when transferring data from the node to the cluster head even though the perfect cluster head was chosen to keep the WSN's energy consumption under control [29]. The distributed cluster approach and the optimistic algorithm were used to find the cluster head in WSNs [30]. The sensors in the network require a power supply to function, so if the batteries in the sensors run out, the wireless sensor network will not function properly. Sensor node battery replacement is a difficult process [20, 31, 32]. The accuracy of location detection can be improved by dividing the total coverage area into multiple grids. The genetic algorithm reduces the number of sensor nodes, ensuring full coverage and maximising energy efficiency and connectivity [21]. It can make the most of its energy by using a fuzzy data fusion method. It uses a fusion spreader framework to improve energy efficiency. The sensor node used more energy when transferring data from the node to the cluster head even though the perfect cluster head was selected to limit the amount of energy used in WSNs where distributed clustering and an optimistic algorithm were used in WSNs [22, 23].

3. Problem Statement and Contribution

Energy consumption is a major consideration in WSNs, as the amount of energy consumed by a node determines how long a network can last. When the nodes are idle, they use less power, but when they begin performing tasks like

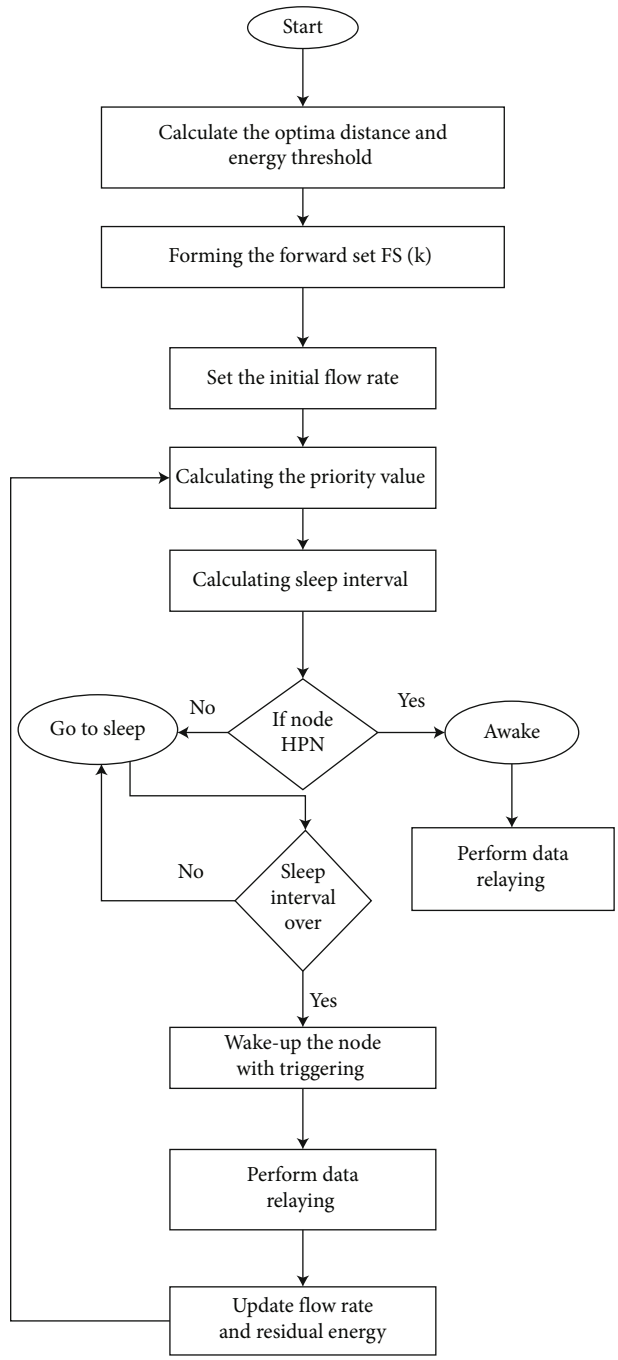

Figure 2: Flow chart for OEERP.

sending data to the cluster head, they use more power and eventually run out of battery life, leading to a death situation. Sensor node energy consumption can be effectively limited if you want to extend the life of WSNs. An opportunistic energy-efficient routing protocol (OEERP) algorithm is presented in this paper to reduce the network's energy usage while routing. It can pinpoint the target with pinpoint accuracy, save energy, and extend the life of the network. To reduce network power consumption, it puts nodes that are not in use into a low-power sleep mode. The major contribution of the OEERP algorithm is given below:

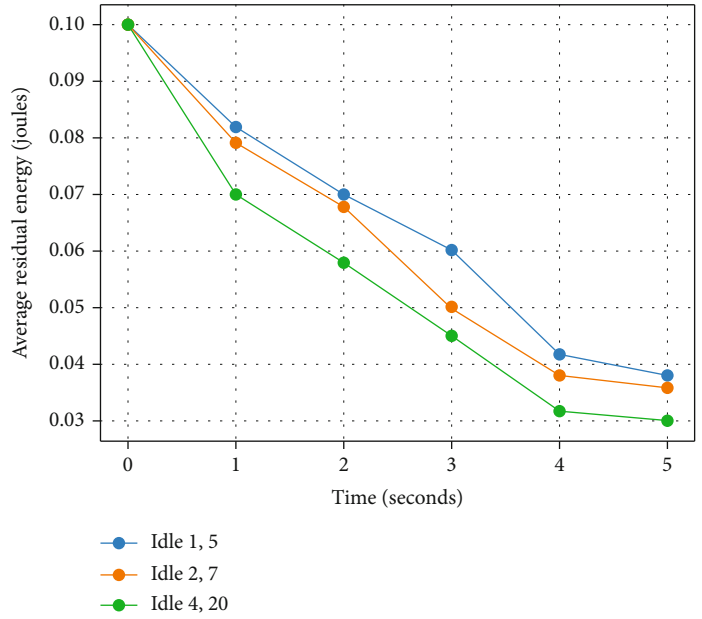

Figure 3: Average of residual energy in the idle state.

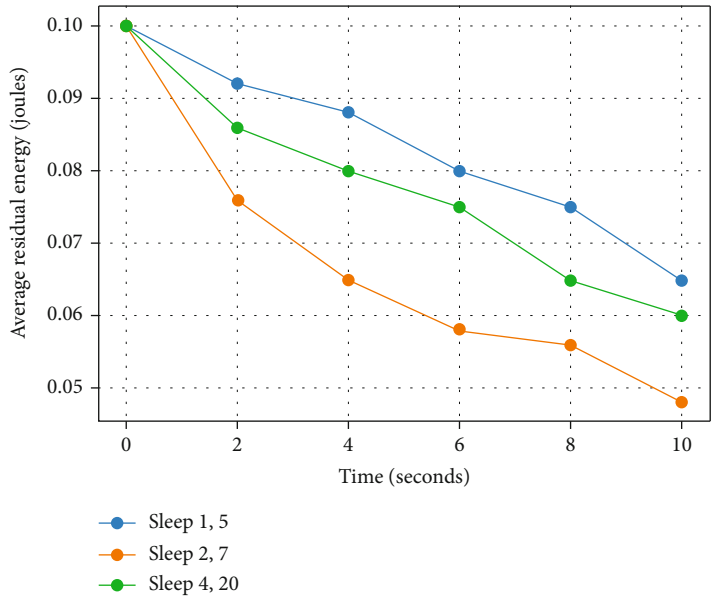

Figure 4: Average of residual energy in the sleep state.

(i) To ensure quality collections of sensor nodes, data are configured and earlier failure states are predicted; consistency sends control commands from the monitor's centre

(ii) It provides self-configurable ability whenever failures are detected, and it finds failure type and degree of impact

(iii) It enables a message notification system; thus, share updating icon information with the subscriber node during quality measures exceeding or below the expected level. Thus, achieve end-to-end node connectivity in real time

(iv) It monitors the system performance after evaluation of past transaction of data with secured device and scales its node coverage range and enhances manageability between sensor nodes

4. Proposed Methodology

The paper proposed the optimistic energy-efficient routing protocol which is used to increase detection of the target

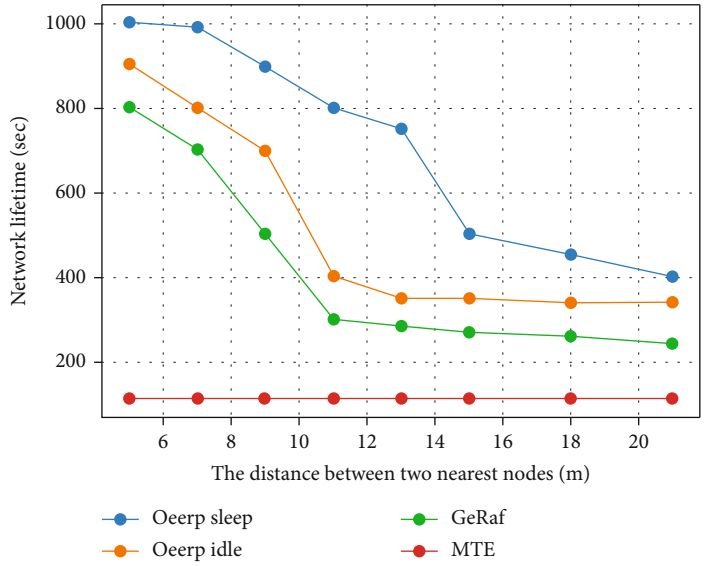

Figure 5: Comparison of a network lifetime with other protocols.

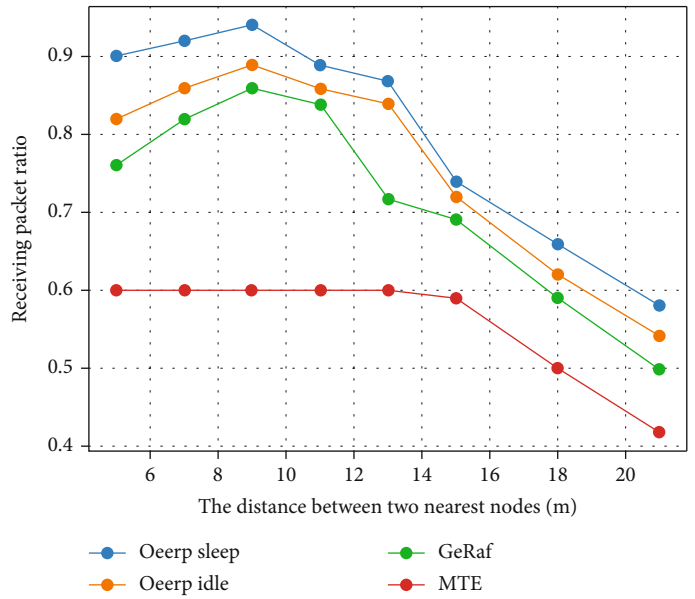

Figure 6: Comparison of RPR with other protocols.

location and the network lifespan, mainly for the energy consumption of the network. The operation of this routing protocol has two types of states: the first one is the sleep state and the second one is the idle state. When the node is in idle mode, put the idle node into the sleep state; in the sleep state, there are 2 modes: initialization mode and sleep/awake based on the sleep scheduling mode. The sleep duration of the nodes depends on the priority value. The sleep mode in the forward set has some time that is given in the equation.

$$TP_x = \sum_{y=1}^{x-1} TP_y. \quad (1)$$

The OEERP is saving the maximum energy when the sink receives the data from the node in the network. While the communication of a network the large amount for energy required of operations. The distribution of energy in the network for a reception of data, for the idle node also the energy will distributed that energy is wasted energy of the networks, to reduce that the OEERP is proposed.

The nodes are not involved in the data relaying process; that is, the nodes are idle nodes. The idle state node also requires the same amount of energy like an active node which is involved in the data relaying process. When calculating the total network's energy consumption, it includes the idle node energy.

The node will perform the transmission and receipt of the data in the network by the given time excluding the idle nodes. The idle node is put into a sleep mode; the algorithm is proposed to reduce the energy. For calculating the energy dissipation in the transmission of an N-bit to the receiver, the distance from transmitter d is given in

$$\mathrm{EDT}_x = \left[\mathrm{SE}_{\mathrm{req}} + \mathrm{AE}_{\mathrm{req}}.d^{\eta}\right]N. \tag{2}$$

The energy consumed by the receiver is given in

$$\mathrm{EDR}_x = \mathrm{SE}_{\mathrm{req}}.N. \tag{3}$$

Calculating the optimum distance for node k is given in equation (4).

When they consider the kth node which started to communicate with the base station if some of the neighbor nodes of kth are also suitable for the same, the neighbor node is selected for the forwarder set; there are so many nodes that will be suitable to become a forwarder set; the node having high priority will become a forwarder set; equation (5) shows the calculation equation for a priority check.

$$\mathrm{Optima}_{\mathrm{dis}} = \frac{Z - x_k}{\mathrm{Optima}_{NH}}. \tag{4}$$

$$\mathrm{PR}_{\mathrm{node}}(k+i) = (d_{k+i} - d_k)\left(\frac{1}{d_{k+i} - \mathrm{Optima}_{\mathrm{dis}}}\right) + (R_x E_{k+i} - E_{Th}). \tag{5}$$

The selected forwarder node will start forwarding the received packets to the next neighboring nodes, the remaining unselected nodes are idle in equation (6), and the OEERP algorithm is proposed to put these idle nodes into a sleep state for consuming energy and increase the node life.

$$\mathrm{TEC}_{\mathrm{idle}} = T_{xE} + R_{xE}N_H + N_{\mathrm{idle}}, \tag{6}$$

$$\mathrm{TEC}_{\mathrm{Sleep}} = T_{xE}N_H + R_{xE}N_H + N_{\mathrm{Sleep}}. \tag{7}$$

When a node is in a sleep state (Nsleep), it will be equal to a zero (Nsleep = 0) energy; then, equation (7) can be written as equation (8).

$$\mathrm{TEC}_{\mathrm{Sleep}} = T_{xE}N_H + R_{xE}N_H, \tag{8}$$

$$\mathrm{Sleep}_{\mathrm{interval}} = \frac{\left(1/d_{hp.od}\right) + \left(R_x E_{kn-1} - E_{Th}\right) - \left(P_{rn}(kn+1)/d_n\right)}{2SE_{\mathrm{req}}B_{\mathrm{rate}} + AE_{\mathrm{req}}B_{\mathrm{rate}}d^{\eta} + E_{\mathrm{idle}}}. \tag{9}$$

All the forwarder set nodes are put into a sleep state which has HPN; the HPN will be awake and performing the data relaying. The sleep time interval is calculated by equation (9).

5. Simulation Results

When a network is active, it consumes more energy than it does when it is idling. Due to the lower power consumption of the relay nodes, this is the case. Table 1 shows the simulation parameters. Figure 2 compares the average residual energy results. A node's residual energy is higher if the node is left idle for a long period of time. This method helps minimise the energy consumption associated with idle listening. Figure 3 depicts the nodes at a 5-meter distance. The energy saving percentage is 66.66 percent for a distance of 7 metres. The remaining energy in the sleep mode is reduced first, and then, that in the idle mode is reduced subsequently. Figure 4 depicts the average residual energy comparison of the results.

OEERP with a sleep mode increases the distance between the nodes as they get closer to each other in the graph shown in Figure 5. This means that the network's lifespan increases as the distance increases. In comparison to other WSNs, the OEERP network has a longer lifespan and uses fewer packets, making it more energy efficient.

Figure 5 shows a network lifetime comparison between the results of the various algorithms. We need to raise the RPR value in order to improve network connectivity. The sleep or idle modes can be used to accomplish this. OEERP with higher RPR initially receives more packets than its peers, as shown in Figure 6. The received packet ratio comparison results of other algorithms are also shown. OEERP's RPR differs from that of other protocols in that the distance between nodes in the sleep mode is 20 metres, increasing the risk of packet loss. An OEERP network in the sleep mode with a higher RPR value will provide a more reliable link to the network.

6. Conclusion

This paper improved the network accuracy of detecting the location of the target, the lifespan, and the energy efficiency. The proposed OEERP algorithm allowed only the forwarder set nodes to the data relaying process. It computes the optimal sleep time for an idle node based on FR and RE. The simulation results show the target detection, the lifespan, and the energy efficiency of the network which is increased in the sleep state than in the idle state, and the performance of the algorithm results is compared with that of other algorithms, namely, GeRaf and MTE. Target detection of the location is based on the received packet ratio; when the received packet ratio is increased, automatically the target detection of the location accuracy will be increased.

Data Availability

The datasets used and/or analyzed during the current study are available from the corresponding author on reasonable request.

Conflicts of Interest

The authors declare that there is no conflict of interest regarding the publication of this paper.

References

[1] K. P. Mhatre and U. P. Khot, "Energy-efficient opportunistic routing with sleep scheduling in wireless sensor networks," *Wireless Personal Communications*, vol. 112, no. 2, pp. 1243–1263, 2020.

[2] H. El Alami and A. Najid, "Optimization of energy efficiency in wireless sensor networks and Internet of Things," *Procedia Computer Science*, vol. 79, pp. 603–609, 2020.

[3] M. Mounika and C. N. Chinnaswamy, "Opportunistic routing protocols for wireless sensor networks: a survey," *International Journal of Computer Science and Information Technologies (IJCSIT)*, vol. 7, no. 2, pp. 928–931, 2016.

[4] N. Chakchouk, "A survey on opportunistic routing in wireless communication networks," *IEEE communications surveys and tutorials*, vol. 17, no. 4, pp. 2214–2241, 2015.

[5] S. Markkandan, S. Sivasubramanian, J. Mulerikkal, N. Shaik, B. Jackson, and L. Naryanan, "Massive MIMO codebook design using gaussian mixture model based clustering," *Intelligent Automation & Soft Computing*, vol. 32, no. 1, pp. 361–375, 2022.

[6] "A novel cluster arrangement energy efficient routing protocol for wireless sensor networks," *Journal of Science and Technology*, vol. 9, no. 2, pp. 1–9, 2016.

[7] K. S. Sankaran, K. Vijayan, S. Yuvaraj et al., "Weighted-based path rediscovery routing algorithm for improving the routing decision in wireless sensor network," *Journal of Ambient Intelligence and Humanized Computing*, 2021.

[8] P. C. S. Reddy and A. Sureshbabu, "An enhanced multiple linear regression model for seasonal rainfall prediction," *International Journal of Sensors, Wireless Communications and Control*, vol. 10, no. 4, pp. 473–483, 2020.

[9] L. Sujihelen, R. Boddu, S. Murugaveni et al., "Node Replication Attack Detection in Distributed Wireless Sensor Networks," *Wireless Communications and Mobile Computing*, vol. 2022, Article ID 7252791, pp. 1–11, 2022.

[10] V. Naranjo, G. Paola, M. Shojafar, H. Mostafaei, Z. Pooranian, and E. J. Baccarelli, "P-SEP: a prolong stable election routing algorithm for energy-limited heterogeneous fog-supported wireless sensor networks," *Journal of Supercomputing*, vol. 73, no. 2, pp. 733–755, 2017.

[11] M. Zorzi and R. R. Rao, "Geographic random forwarding (GeRaf) for ad hoc and sensor networks: energy and latency performance," *IEEE Transactions on Mobile Computing*, vol. 2, no. 4, pp. 349–365, 2003.

[12] X. Mao, S. Tang, X. Xu, X. Y. Li, and H. Ma, "Energy-efficient opportunistic routing in wireless sensor networks," *IEEE Transactions on Parallel and Distributed Systems*, vol. 22, no. 11, pp. 1934–1942, 2011.

[13] D. Liu, Z. Zheng, Z. Yuan, and W. Li, "An improved TPSN algorithm for time synchronization in the wireless sensor network," in *In 32nd international conference on distributed computing systems workshop*, pp. 279–284, Macau, China, 2012.

[14] M. A. A. Da Cruz, J. J. P. C. Rodrigues, J. Al-Muhtadi, V. V. Korotaev, and V. H. C. Albuquerque, "A reference model for Internet of Things middleware," *IEEE Internet of Things Journal*, vol. 5, no. 2, pp. 871–883, 2018.

[15] A. Singhal, S. Varshney, T. A. Mohanaprakash et al., "Minimization of latency using multitask scheduling in industrial autonomous systems," *Wireless Communications and Mobile Computing*, vol. 2022, Article ID 1671829, pp. 1–10, 2022.

[16] P. C. S. Reddy, S. Yadala, and S. N. Goddumarri, "Development of rainfall forecasting model using machine learning with singular spectrum analysis," *IIUM Engineering Journal*, vol. 23, no. 1, pp. 172–186, 2022.

[17] J.-S. Lee and C.-L. Teng, "An enhanced hierarchical clustering approach for mobile sensor networks using fuzzy inference systems," *IEEE Internet of Things Journal*, vol. 4, no. 4, pp. 1095–1103, 2017.

[18] D. Balamurugan, S. S. Aravinth, P. C. S. Reddy, A. Rupani, and A. Manikandan, "Multiview objects recognition using deep learning-based Wrap-CNN with voting scheme," *Neural Processing Letters*, vol. 54, no. 3, pp. 1495–1521, 2022.

[19] H. Subash and K. Pratyay, "Coverage and connectivity aware energy efficient scheduling in target based wireless sensor networks: an improved genetic algorithm based approach," *Network*, vol. 25, no. 4, pp. 1995–2011, 2019.

[20] A. M. Mohan, C. G. Mahesh, S. Madhavi, and G. Saurabh, "Fuzzy based data fusion for energy efficient Internet of Things," *International Journal of Grid and High Performance Computing*, vol. 11, no. 3, pp. 46–58, 2019.

[21] F. Hanlin and C. Zhiwei, "Target tracking based on improved square root cubature particle filter via underwater wireless sensor networks," *IET Communications*, vol. 13, no. 8, pp. 1008–1015, 2019.

[22] C. Huayan, Z. Senlin, L. Meiqin, and Z. Qunfei, "An artificial measurements-based adaptive filter for energy-efficient target tracking via underwater wireless sensor networks," *Sensors*, vol. 17, no. 5, p. 971, 2017.

[23] F. Juan, S. Xiaozhu, and Z. Jinxin, "Dynamic cluster heads selection and data aggregation for efficient target monitoring and tracking in wireless sensor networks," *International Journal of Distributed Sensor Networks*, vol. 14, no. 6, 2018.

[24] E. Alami, "EEA," *International Journal of Wireless Networks and Broadband Technologies (IJWNBT)*, vol. 7, no. 2, pp. 19–37, 2018.

[25] X. Lida, "Internet of Things in industries: a survey," *IEEE Transactions on Industrial Informatics*, vol. 10, no. 4, pp. 2233–2243, 2014.

[26] L. Guiyun and X. Bugong, "Novel sensor scheduling and energy-efficient quantization for tracking target in wireless sensor networks," *Journal of Control Theory and Applications*, vol. 11, no. 1, pp. 116–121, 2013.

[27] J.-S. Lee and W.-L. Cheng, "Fuzzy-logic-based clustering approach for wireless sensor networks using energy predication," *IEEE Sensors Journal*, vol. 12, no. 9, pp. 2891–2897, 2012.

[28] P. Lorenza and H. A. Mohammad, "An energy-efficient predictive model for object tracking sensor networks," in *2019. In: IEEE 5th world forum on Internet of things*, pp. 15–18, Limerick Ireland, 2019.

[29] Q. Yifei, P. Cheng, B. Jing, C. Jiming, G. Adrien, and S. Yeqiong, "Energy-efficient target tracking by mobile sensors with limited sensing range," *IEEE Transactions on Industrial Electronics*, vol. 63, no. 11, pp. 6949–6961, 2016.

[30] L. Jing, Y. Xiaofeng, and L. Huiyong, "Collaborative energy-efficient moving in Internet of Things: genetic fuzzy tree vs. neural," *Network*, vol. 14, no. 8, 2015.

[31] S. Chao, Z. Lianhua, Y. Bian, S. Dandan, and R. Chunhui, "A type of energy-efficient target tracking approach based on grids in sensor networks," *Peer-to-Peer Networking and Applications*, vol. 12, no. 5, pp. 1041–1060, 2019.

[32] E. Alami and A. Najid, "(SET) smart energy management and throughput maximization," *Security Management in Mobile Cloud Computing*, 2017.

[33] Y. Liu, B. Xu, and L. Feng, "Energy-balanced multiple-sensor collaborative scheduling for maneuvering target tracking in wireless sensor networks," *Journal of Control Theory and Applications*, vol. 9, no. 1, pp. 58–65, 2011.

[34] K. Atia George, V. Veeravalli Venugopal, and J. A. Fuemmeler, "Sensor scheduling for energy-efficient target tracking in sensor networks," *IEEE Trans Signal Process*, vol. 59, no. 10, pp. 4923–4937, 2011.